Coordinated EISCAT Svalbard radar and Reimei satellite observations of ion upflows and suprathermal ions

Coordinated EISCAT Svalbard radar and Reimei satellite observations of ion upflows and suprathermal ions

Y. Ogawa,[1] K. Seki,[2] M. Hirahara,[3] K. Asamura,[4] T. Sakanoi,[5] S. C. Buchert,[6] Y. Ebihara,[7] Y. Obuchi,[5] A. Yamazaki,[4] I. Sandahl,[8] S. Nozawa,[2] and R. Fujii[2]

[1]   The relationship between bulk ion upflows and suprathermal ions was investigated using data simultaneously obtained from the European Incoherent Scatter (EISCAT) Svalbard radar (ESR) and the Reimei satellite. Simultaneous observations were conducted in November 2005 and August 2006, and 14 conjunction data sets have been obtained at approximately 630 km in the dayside ionosphere. Suprathermal ions with energies of a few eV were present in the dayside cusp region, and the ion velocity distribution changed from an isotropic Maxwellian near the cusp region to tail heating at energies above a few eV in the cusp region. The velocity distribution of the suprathermal ions has a peak perpendicular or oblique to the geomagnetic field, and the temperature of the suprathermal ions was 0.9–1.4 eV. An increase in the phase space density (PSD) of the suprathermal ions, measured with the Reimei, was correlated with bulk ion upflow observed at the same altitude using EISCAT, and with the energy flux of precipitating electrons with energies of 50–500 eV. The PSD also has a good correlation with the electron temperature, which was increased by precipitation, but not with the ion temperature (0.1–0.3 eV) at the same altitude measured with EISCAT. These results suggest that plasma waves such as broadband extremely low frequency (BBELF) wavefields associated with precipitation are connected to the bulk ion upflows in the cusp and effectively cause the heating of suprathermal ions. The heating of suprathermal ions disagrees with anisotropic heating due to O^+-O resonant charge exchange.

1.   Introduction

[2]   Over the past few decades a considerable number of studies have been made on ion outflow from the polar ionosphere to the magnetosphere. The outflow of ions is a significant source of magnetospheric plasma, and also affects the dynamics of the magnetosphere. On the basis of several observations around the bottomside magnetosphere, ion outflow phenomena in the auroral zone and dayside cusp region can be divided into several types, such as ion beams, transversely accelerated ions (TAIs), ion conics, and upwelling ions (UWIs). Transverse ion heating events with typical energies from thermal to a few keV, called TAIs, are accompanied with upward flowing ions, electron precipitation and density depletions, and a variety of different resonant waves, such as lower hybrid (LH) waves or broadband extremely low frequency (BBELF) waves [*Moore et al.*, 1996; *Lynch et al.*, 1996; *Kintner et al.*, 1996; *André*, 1997; *Frederick-Frost et al.*, 2007]. A statistical study using data from the Freja satellite obtained near 1700 km altitude shows that BBELF waves are the most common wave signatures associated with perpendicular O^+ ion heating to mean energies above 5–10 eV, in particular in the cusp region [*Norqvist et al.*, 1996; *André et al.*, 1998]. Large-amplitude electric field fluctuations of BBELF waves can accelerate ionospheric ions in the perpendicular plane [e.g., *Lundin and Hultqvist*, 1989; *Hultqvist*, 1996].

[3]   Around the auroral oval and cusp region, bulk ions in the F region/topside ionosphere move upward along the field lines with transient plasma heating [e.g., *Wahlund et al.*, 1992; *Ogawa et al.*, 2003]. This phenomenon is called ion upflow. Ion upflow is often observed with incoherent scatter (IS) radars located at high latitudes [e.g., *Keating et al.*, 1990; *Foster et al.*, 1998; *Endo et al.*, 2000]. The typical velocity of ion upflow is a few 100 m s^{-1} to a few 1000 m s^{-1}, which is smaller than the escape velocity from the Earth. Hence it is still not understood how the ion upflow at high latitudes

[1]National Institute of Polar Research, Tokyo, Japan.
[2]Solar-Terrestrial Environment Laboratory, Nagoya University, Nagoya, Japan.
[3]Department of Physics, College of Science, Rikkyo University, Tokyo, Japan.
[4]Institute of Space and Astronautical Science, Japan Aerospace Exploration Agency, Kanagawa, Japan.
[5]Planetary Plasma and Atmospheric Research Center, Graduate School of Science, Tohoku University, Miyagi, Japan.
[6]Swedish Institute of Space Physics, Uppsala, Sweden.
[7]Institute for Advanced Research, Nagoya University, Nagoya, Japan.
[8]Swedish Institute of Space Physics, Kiruna, Sweden.

relates to the magnetospheric ion outflow for which the ions have presumably overcome the Earth's gravity and succeeded to escape. However, ion upflow must certainly play an important role as a plasma source of the ion outflow, because heavy ions such as NO^+ and O_2^+, which are found in the ion outflow and in the magnetosphere, should primarily exist only in the lower ionosphere. Therefore a certain process must occur, such as ion upflow, to bring these heavy ions to the bottomside magnetosphere.

[4] Although both ion upflow and TAIs occurring in the vicinity of the auroral zone and cusp region are related to soft electron precipitation, the relationships between bulk ion upflows, thermal ion heating, and TAIs are not yet fully understood. Therefore an obvious question is how the bulk ion upflow is related to the heating associated with TAIs, which are often observed at somewhat higher altitudes as well as at higher transverse energies. Freja satellite observations at altitudes between 1100 and 1600 km have shown that perpendicular energization (>0.5 eV) events were associated with bulk ion upflows, derived using an energy filter at 3.5 eV on the two neighboring mass spectrometer (TICS) instruments [*Norqvist et al.*, 1998]. However, it was difficult to derive the thermal ion temperature correctly during TAI events. Generally, it is difficult to find such characteristics only with a single measurement (i.e., Incoherent Scatter radar or satellite).

[5] We have therefore conducted coordinated European Incoherent Scatter (EISCAT) Svalbard radar (ESR) and Reimei observations, to investigate the relationship between thermal and suprathermal ion behavior in the dayside polar ionosphere. The coordinated observations were conducted in November 2005 and August 2006, and 14 conjunction data sets have been obtained simultaneously in the dayside ionosphere at an altitude of approximately 630 km. In this paper, we will show results of the direct comparison of the energization of thermal and suprathermal ions.

2. Instruments and Simultaneous Observations

2.1. Reimei Satellite

[6] The Reimei satellite, launched from the Baikonur Cosmodrome in Kazakhstan on 23 August 2005, orbits the Earth at an altitude of approximately 630 km with an orbital inclination of 98.6 deg [*Saito et al.*, 2005]. In order to investigate the fine structure and variations of auroral phenomena, the Reimei satellite carries five scientific instruments: top-hat-type auroral electron and ion energy spectrum analyzers (ESA and ISA) [*Asamura et al.*, 2003], a three channel monochromatic auroral imaging CCD camera (MAC) [*Sakanoi et al.*, 2003], current probes (CRM) and magnetic field sensors (GAS). Two-dimensional distribution functions of ions/electrons in the energy range of 10 eV/q to 12 keV/q divided by 32 logarithmic steps, are obtained from ESA/ISA. The time resolution of the ESA/ISA is 40 ms for one 2-d distribution function, which corresponds to a horizontal spatial scale of 300 m.

[7] The Reimei is a sun synchronous satellite, and the meridian plane of the orbit is 0050–1250 local time (LT). The Reimei passes over Svalbard at approximately 04 and 10 LT every day, corresponding to approximately 06 and 12 magnetic local time (MLT). Therefore there are several good opportunities to simultaneously observe the dayside

cusp phenomena with both the Reimei satellite and the EISCAT Svalbard radar.

2.2. Eiscat Svalbard Radar

[8] The EISCAT radars, located in Northern Scandinavia and Svalbard, measure ionospheric parameters, such as plasma density, temperature, and velocity at altitudes between approximately 80 and 1000 km, which covers the height of the Reimei satellite (approximately 630 km). The EISCAT Svalbard radar (ESR), located in Longyearbyen Svalbard, has 2 antennae, a 32 m steerable dish and a 42 m fixed dish, and is a suitable tool for observation of the dayside cusp phenomena, because of its location (geographic latitude: 78.15 deg N, geographic longitude: 16.02 deg E, invariant latitude: 75.18 deg). Field-aligned ion upflows are frequently observed around the cusp region using the ESR 42 m dish.

[9] Since the cusp region, including cusp proper and boundary cusp, has a longitudinally elongated shape [*Newell and Meng*, 1992; *Maynard et al.*, 1997], simultaneous ESR and Reimei data have been selected where the Reimei satellite passes within 350 km (equivalent to a span of 1 h MLT) from the magnetic field line of the ESR during the time period when the ESR is located between 1000 and 1400 MLT. The MLT is UT + 3 h. For coordinated observations, the ESR 32 m dish was directed to the nearest point of the satellite orbit from the radar, so that we were able to measure a common volume at the same time with both ESR and Reimei. We have confirmed that ionospheric conditions, such as ion/electron heating in the topside ionosphere, did not change between the data from the ESR 42 m and 32 m dishes, when the Reimei satellite passed near the ESR 32 m beam.

[10] Simultaneous ESR and Reimei observations were conducted in November 2005 and August 2006, and 14 conjunction events were obtained. First, we give a detailed presentation of one event where the bulk ion upflow seems to be related to suprathermal ions. Next, a total of 14 events are then used in a statistical study of ion heating mechanisms.

3. Results

3.1. A Case Study on 8 August 2006

[11] Figure 1 shows the Nadir ground track of the Reimei satellite between 0903 and 0907 UT on 8 August 2006. The Reimei satellite moved from low to high latitude at an altitude of 632 km, and intersected the cusp region. For this event we used only the ESR 42 m dish to obtain field-aligned data, because the predicted orbit of Reimei was within the ESR 42 m beam. The closest approach of Reimei to the ESR was at 0904:24 UT, which is at approximately 1148 magnetic local time (MLT).

[12] One day before this conjunction event, a magnetic storm occurred. Geomagnetic activity was relatively high with the *Kp* index = 3 and *Dst* index = −28 during the conjunction event. The interplanetary magnetic field (IMF) changed from approximately 0 to −3.5 nT at the ACE spacecraft's location (the Lagrangian point L1) at approximately 0730 UT on 8 August. The solar wind velocity and density, measured with the ACE, were approximately 600 km s^{-1} and 2.4 cc^{-1}, respectively.

[13] Figure 2 shows the time variations of the ionospheric plasma parameters along the local geomagnetic field line, measured with the ESR 42 m dish between 0835
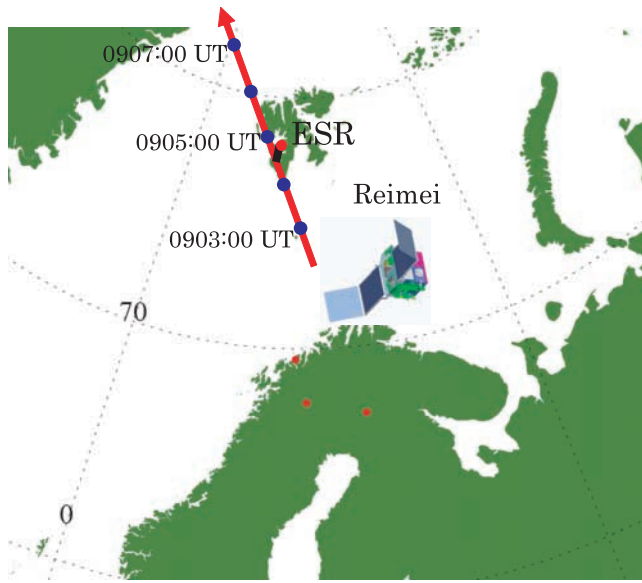
Figure 1. Nadir ground track of the Reimei satellite between 0903 and 0907 UT on 8 August 2006. The Reimei satellite intersected the cusp region at 632 km altitude.

and 0932 UT on 8 August 2006. Continuous electron heating (Figure 2b) and ion upflows (Figure 2d) were seen at the beginning of the observation until 0920 UT. When the electron temperature is high above an altitude of 400 km, the electron density (Figure 2a) increases at an altitude of 200–300 km due to soft particle precipitation. The ion temperature was high between 0854 and 0900 UT, but became low at the conjunction time (at 0904 UT, denoted by a red bar in Figure 2).

[14] At the conjunction time, the upward ion velocity and the electron temperature were approximately 500 m s^{-1} and 3500 K, respectively, at the Reimei altitude. Just before and after the conjunction (08:50 and 0912 UT, respectively), the electron temperature exceeded 6000 K above 500 km altitude, and naturally enhanced ion-acoustic lines (NEIALs) were observed at approximately 500 km altitude. It should be noted that the plasma parameters were derived after removing such enhanced lines.

[15] Figure 3 shows electron and ion energy spectra measured with Reimei ESA/ISA between 0903:55 and 0904:35 UT. They are, from top to bottom, downward (0–30 deg), perpendicular (60–120 deg) and upward (150–180 deg) electrons, and then downward, perpendicular and upward ions, respectively. The cusp is characterized by a strong peak in the downward ion energy flux at ∼1 keV and high ion number fluxes (Figure 3d). Soft electron precipitation (<500 eV) is also typically observed in the cusp (Figure 3a). The cusp signature was seen in the Reimei data between 0904:05 and 0904:25 UT. Electron precipitation was also seen with peak energies of 100–200 eV between 0903:56 and 0904:25 UT, at almost the same time as the ion precipitation. The precipitation of electrons is rather intermittent equatorward of the cusp between 0903:55 and 0904:05 UT, and also at the poleward edge of the cusp around 0904:27 UT.

[16] A notable characteristic is the existence of low energy (<50 eV) ions in the direction perpendicular to the magnetic field (see Figure 3e). The low energy ions (<50 eV) were seen from 0904:02 UT until 0904:29 UT, and temporal/spatial variation of the low energy ions seems to be correlated to that of the precipitating electrons at 10–500 eV. Although this variability is seen, the latitudinal width of the low energy ions is more than 1 deg (77.3–78.6 deg), corresponding to a distance of more than 100 km. The location of the simultaneous observation was near the poleward edge of the cusp at 0904:24 UT (denoted by a red bar in Figure 3).

[17] Figure 4 shows the ion distribution function derived from the Reimei ISA at 0904:24 UT when the Reimei passed into the ESR beam. The data at the pitch angles between 0 and −85 deg are missing because of shading by the solar panel. The phase space density (PSD), *F*, was derived using the following equation,

$$F(v) = \left(\frac{C}{\tau}\right)\left(\frac{m^2}{2\varepsilon g E^2}\right) \qquad (1)$$

where *C* is counts, τ is the sampling time, *m* is the ion mass, ε is the detection efficiency, *g* is a geometric factor, and *E* is energy. In order to obtain reliable PSD, the Reimei ISA data were accumulated for 0.4 s, corresponding to 3 km in horizontal distance and almost one half of the ESR beam width (the beam width is 6.7 km at 630 km altitude).

[18] The pitch angle (PA) distribution of ions with energies between 50 eV and 5 keV is wide (±100 deg). The PA distribution of electrons with energies between 100 and 500 eV is also wide, ±100 deg (not shown here).

[19] As mentioned regarding Figure 3, there are many counts of low energy ions (less than 50 eV) perpendicular to the magnetic field. The low energy ions appearing in the perpendicular direction have PAs between 90 and 150 degrees, and the angle of the PSD peak is 116 deg. For the low energy ions, the satellite ram direction projected to the instrumental field of view (FOV) surface has to be taken into account (the ram direction is shown in the center of the Figure 4a, using a blue solid bar). The ram direction PA and the satellite velocity are 95 deg and 7.6 km s^{-1}, respectively.

[20] Assuming that the low energy ions are protons, and taking into account the satellite velocity of 7.6 km s^{-1}, the ion flux should also appear in the PA direction between −90 and −150 deg. In contrast, if oxygen ions are assumed, they would not appear in the anti-ram direction because their ram energy in the spacecraft frame is below the detector threshold. The observed ions are concluded to be heavy ions, probably oxygen ions, since there are no ions in the anti-ram direction.

[21] In Figure 4b we plotted the PSD of ions at the same time (0904:24 UT), but corrected for the ram effect assuming that the low energy ions are oxygen ions. The low energy (10 eV) ions perpendicular to the magnetic field (90 and 150 degrees) in Figure 4a, are shown in the smaller energy (2–4 eV) in Figure 4b. Also, ions parallel to the magnetic field (PA: ∼180 deg) are now seen at energy of about 10 eV in Figure 4b. The number of upward ions (PA: ∼180 deg) is larger than that of downward ions (PA: ∼0 deg)

[22] Figure 5 shows the comparison between the ion distributions derived from the ESR and the low energy ions measured by Reimei at the same time (0904 UT) and
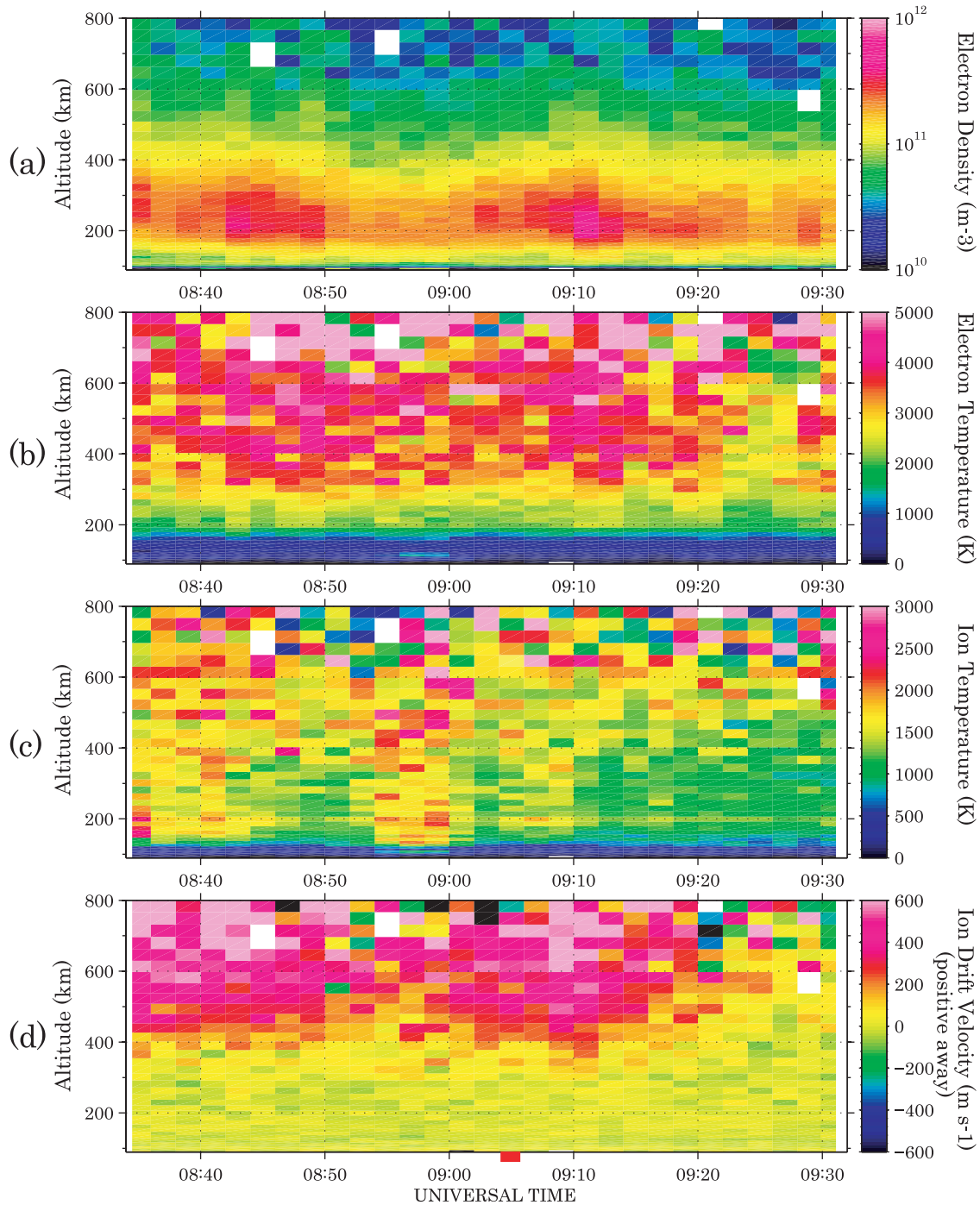
Figure 2. Time variations of the ionospheric plasma parameters along the local geomagnetic field line, measured with the EISCAT Svalbard radar (ESR) 42 m fixed dish between 0835 and 0932 UT on 8 August 2006. The closest approach of the Reimei satellite to the ESR is denoted by a red bar.

position at 630 km altitude. The red dashed lines indicate the ion distribution function measured with ESR (using $Ne = 4.1 \times 10^{10}$ m^{-3}, $Ti_{//} = 1675$ K). The ESR data were obtained assuming Maxwellian distributions of ions and electrons, and 100% oxygen ions at 630 km altitude. The ESR data were integrated for 2 min, while the ESR was directed along the geomagnetic field line. The red thin dashed lines at upper and lower parts of the red thick dashed line indicate that the errors of Incoherent Scatter (IS) spectra

fitting ($\Delta Ne = 3.7 \times 10^{9}$ m^{-3}, $\Delta Ti_{//} = 204$ K) are taken into account.

[23] The light blue solid line indicates the ion distribution function derived from the Reimei ISA data with a PA of 116 deg and 0.4 s integration at the same time (0904:24 UT). The black dashed line indicates a Maxwellian distribution function inferred from the suprathermal ions (4–8 eV) observed with Reimei ISA. The density and temperature, used for the Maxwellian distribution function, were $6.4 \times$
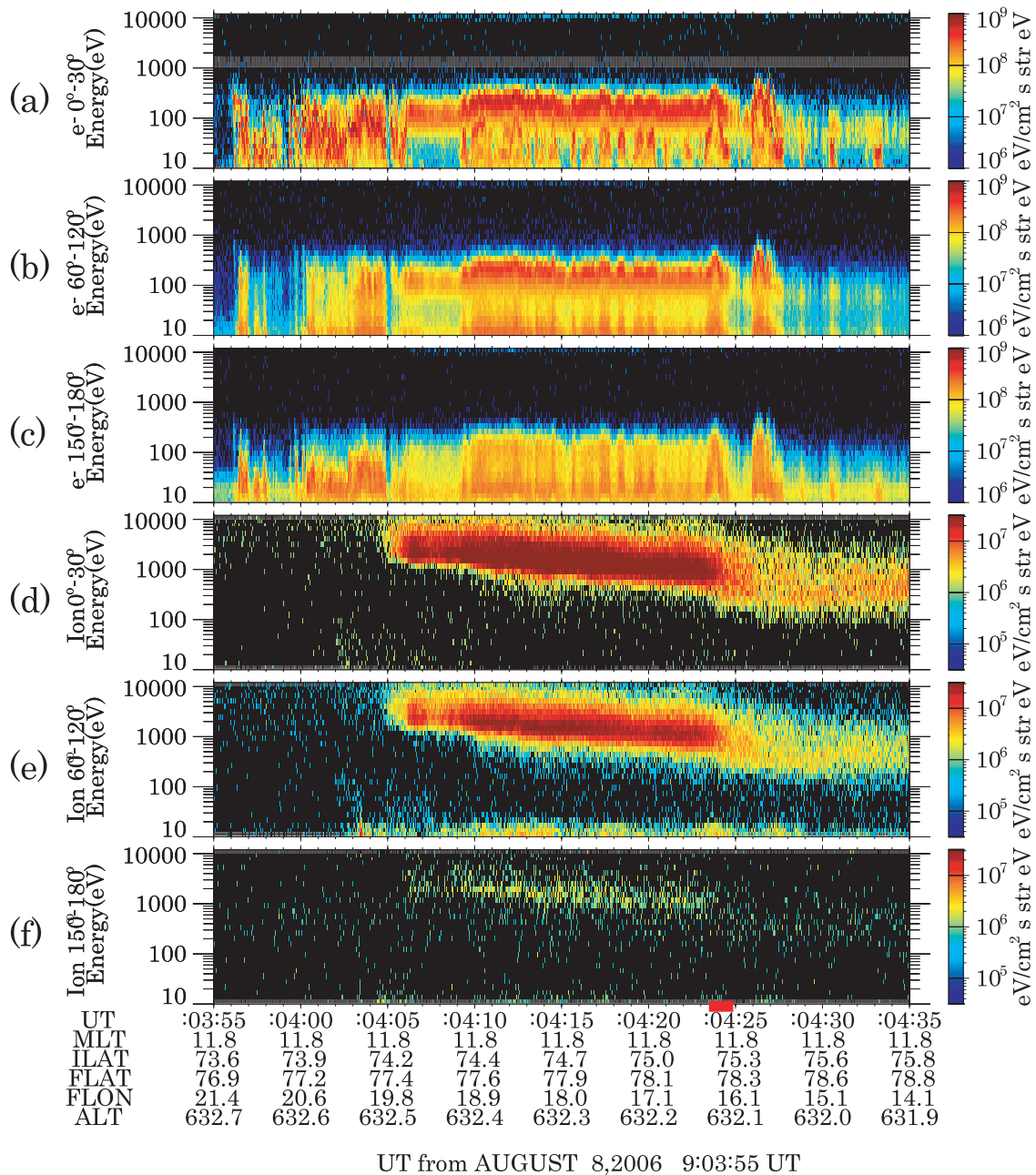
REIMEI EISA (Level 2)

Figure 3. Electron and ion energy spectra measured with the Reimei ESA/ISA between 0903:55 and 0904:35 UT (1148 MLT) on 8 August 2006. The closest approach of the Reimei satellite to the ESR is denoted by a red bar.

10^7 m^{-3} and 11,000 K ($\sim$0.9 eV), respectively. The average temperature of 11,000 K inferred from the Reimei ISA data is approximately 7 times larger than the average ion temperature (1675 K) in the ionosphere. The results indicate that the ion temperatures measured with ESR and Reimei differ in regards to energization.

3.2. Statistical Results

[24] In order to quantitatively investigate the relation between the ion upflow and the low energy suprathermal ions, the 14 events were used in a statistical study of the ion

heating mechanisms. The event times are listed in Table 1. All the ESR data were integrated for 2 min, and the Reimei data for 0.4 s. We have also confirmed that choice of the integration time has not affected the statistical characteristics of the ion upflows, suprathermal ions, and precipitating electrons, by repeating the calculation with a doubled integration time (0.8 s) for the Reimei data.

[25] Figure 6 shows the relationship between field-aligned (FA) ion upflow and the electron/ion temperature. The FA ion velocities and temperatures are derived with the ESR 42 m data. Upward bulk ion upflow is well correlated to the
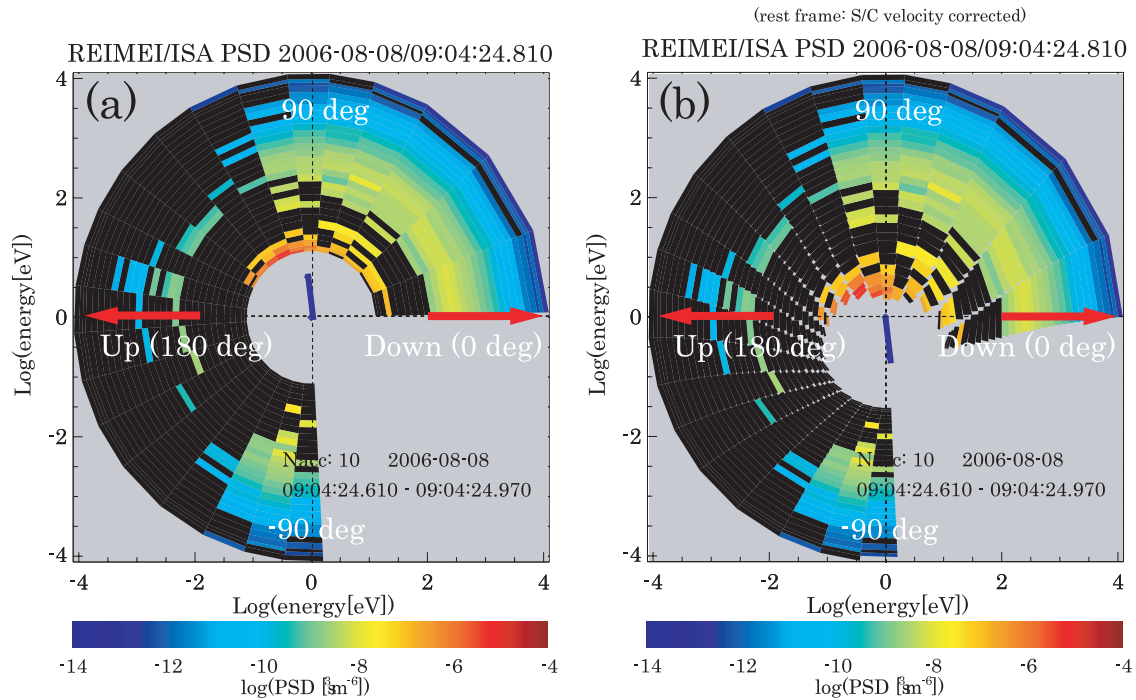
Figure 4. (a) Ion distribution function from the Reimei ISA at 0904:24 UT on 8 August 2006. (b) The same function as (a), but assuming that the low energy ions are oxygen ions and taking the ram effect into account.

electron temperature in the cusp region (see Figure 6a). When the electron temperature was more than 4500 K at 630 km altitude, the ion velocity exceeded 700 m s^{-1} at the same altitude. Ion upflow events (>500 m s^{-1}) were seen in the cusp region, while other samples with an ion velocity of less than 200 m s^{-1} were located mainly equatorward of the cusp region.

[26] The phase space density (PSD) of suprathermal ions, with an energy of 3 eV in a direction nearly perpendicular to the magnetic field (116 deg), were derived from the Reimei ISA measurements after being corrected for ram velocity, and are classified into four groups (red, yellow, blue, and black) based on the PSD value at 3 eV, 116 deg pitch. The suprathermal ion distributions always have a peak at the direction perpendicular or obliquely upward to the magnetic field. However, it was not feasible to calculate the bulk upflow velocity from the Reimei moment because of limitations of Reimei ISA. The temperatures derived from the suprathermal ion distributions were 0.9–1.4 eV. Increase of the PSD was clearly correlated with the upward bulk ion velocity (see Figure 6a). The electron temperature, as well as the upward bulk ion velocity, was also clearly correlated with suprathermal ion enhancements.

[27] On the other hand, there was no clear correlation between upward bulk ion velocity and ion temperature (see overlaid color signatures on Figure 6b). There was also little correlation between the ion temperature and suprathermal ions enhancements. Even when suprathermal ions appeared, the ion temperatures were sometimes less than 2000 K (corresponding to 0.17 eV).

[28] Figure 7 shows the relationship between precipitating electron energies seen by Reimei and ion upflows seen by ESR at approximately 630 km altitude. Precipitating

electron energies are divided into 4 categories: 50–100 eV, 100–300 eV, 300–500 eV, and 1000–12,000 eV. A clear correlation between the energy fluxes of low energy precipitating electrons (50–100 eV, 100–300 eV, and also 300–500 eV electrons) and bulk ion upflows was observed. When the upward ion velocity exceeds 200 m s^{-1}, soft electron precipitation with energies of 50–100 eV were >10^9 eV cm^{-2} s^{-1}, and precipitation of 100–300 eV (300–500 eV) were >10^{10} eV cm^{-2} s^{-1} except for 1 sample (2 samples). The soft electron precipitation with energies of 50–300 eV correlated closely with electron temperature at 630 km altitude (not shown here). This is because soft electron precipitation is often accompanied by the downward heat flux of electrons from the magnetosphere. The energy flux of more than 1 keV electrons is also high (sometimes above 10^{10} eV cm^{-2} s^{-1}), but there is no clear correlation between the energy flux and the upward bulk ion velocity.

4. Discussion

[29] The simultaneous and co-located EISCAT Svalbard radar (ESR) and Reimei observations show that the increase of suprathermal ions with energies of a few eV, and the energy flux of precipitating electrons with energies of 50–500 eV, are associated with FA ion upflows, as well as enhancements of the electron temperature. In the cusp region, the suprathermal ions are seen in directions perpendicular and oblique to the magnetic field, and sometimes upward along the magnetic field. Ion temperatures derived from the distribution of suprathermal ions were 0.9–1.4 eV. The velocity distribution of the suprathermal ions is not smoothly connected to the velocity distribution measured with the ESR, because the ion temperatures from the ESR were 0.1–0.3 eV at the same time and altitude (630 km). The
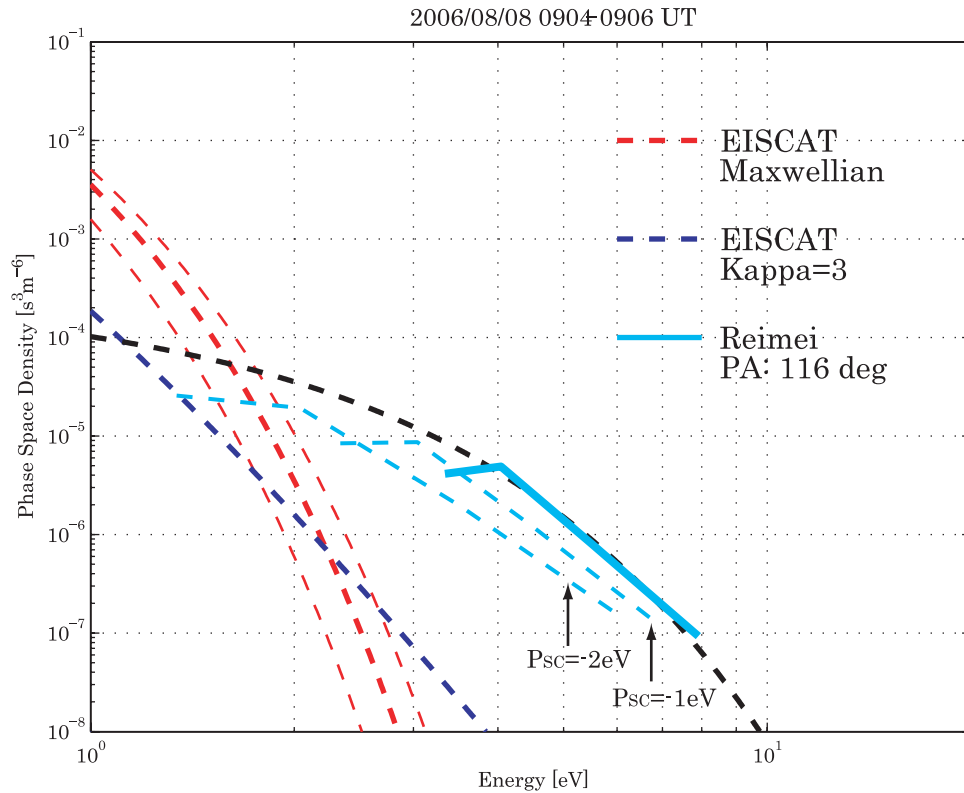
Figure 5. Comparison between the ion distributions derived from the ESR and the low energy ions measured by the Reimei satellite at the same time and position at 630 km altitude. The red dashed line indicates the ion distribution function derived from the ESR data ($Ne = 4.1 \times 10^{10}$ m^{-3}, $Ti_{\parallel} = 1675$ K). The purple dashed line indicates that for ions with a kappa distribution function assuming $\kappa = 3$ and the Ne and Ti are the same values as the ESR data. The light blue line is derived from the Reimei ISA data (PA: 116 deg), and the black dashed line is that inferred from the ion velocity distribution function from Reimei (6.4×10^7 m^{-3} and 11,000 K). The light blue dashed lines are taking the spacecraft potential into account (-1 and -2 eV, respectively).

recent results of comparison between the SERSIO rocket and ESR data also showed that FA ion upflows in the cusp region were accompanied with enhancements of the suprathermal ions typically seen above 3 eV [*Frederick-Frost et al.*, 2007]. The ion temperatures derived from the in situ measurement on the rocket were sometimes more than 5000 K (>0.4 eV) above 700 km altitude in the cusp region, whereas the ion temperature measured with the ESR was approximately 2000 K [*Frederick-Frost et al.*, 2007]. In this section we discuss what causes the inconsistency of the ion temperatures.

[30] The ESR observes only the FA ion temperature. The temperature (<0.4 eV) measured with the radar in the ionosphere is not necessarily isotropic. For example, the ion temperature perpendicular to the magnetic field can be higher than the FA temperature in the cusp region. A previous study using simultaneous ESR and EISCAT Tromsø VHF data at an altitude of 665 km shows that, in the cusp region, significant ion temperature anisotropy, increases of the ion temperature obliquely to the magnetic field line, and small decreases of the FA ion temperature are associated with FA ion upflows, as well as isotropic enhancements of the electron temperature [*Ogawa et al.*, 2000]. If we assumed a higher ion temperature perpendicular to the magnetic field, the ion distribution func-

tion would agree better with that obtained from the Reimei. However, an anisotropy still cannot explain such a high temperature (~1.0 eV), because the expected ratio of the ion temperature anisotropy is approximately 2 [*Ogawa et al.*, 2000].

[31] The Reimei ISA data we used were accumulated for 0.4 s, corresponding to 3 km in horizontal distance and almost one half of the ESR beam width (6.7 km at 630 km altitude). Therefore both Reimei and ESR show spatial averages over comparable sizes. The low energy ions exist in the whole cusp region (see Figure 3e, for example), and therefore our choice of the integration time of the Reimei data did not affect statistical characteristics. Also the time resolutions of the two measurements were different. The ESR averaged over longer time, 2 min, than Reimei, 0.4 s. Possibly heated ion distributions existed over a shorter period than the integration time of the ESR, and therefore the temperatures might be somewhat underestimated and smoother compared to than those derived from Reimei.

[32] When deriving ion temperatures from Reimei ISA data, we may take into account effects from a nonzero satellite potential. The satellite can be charged to minus a few V, according to the data from the thermal ion detectors on SERSIO rocket [*Frederick-Frost et al.*, 2007]. If Reimei was charged negatively, the ion density estimated from ISA data

Table 1. Simultaneous Events of ESR and Reimei Observations

02 Nov 2005, 09:35 UT
03 Nov 2005, 08:20 UT
03 Nov 2005, 09:53 UT
04 Nov 2005, 08:36 UT
04 Nov 2005, 10:13 UT
05 Nov 2005, 07:20 UT
05 Nov 2005, 08:54 UT
06 Nov 2005, 09:14 UT
06 Nov 2005, 10:50 UT
03 Aug 2006, 09:06 UT
08 Aug 2006, 09:04 UT
18 Aug 2006, 08:59 UT
19 Aug 2006, 09:18 UT
20 Aug 2006, 09:37 UT

becomes smaller and the ion temperature gets slightly larger, increasing the difference to the ESR value (see dashed light blue lines in Figure 5). Therefore it seems impossible to get a satisfying agreement between the distributions fitted to ESR and satellite data by assuming negative charging of the spacecraft, even rather large one. If the ion velocity distribution is assumed to be rather a kappa distribution with the same temperature as obtained with the Maxwellian fit, but which is enhanced at high energies compared to a Maxwellian, then the inclination of the distribution function from the ESR (see the purple dashed line in Figure 5) would be closer to that of the distribution above 2 eV from Reimei. However, when the distribution from Reimei ISA data are fitted using the kappa distribution function, a very high ion density much higher than 10^{12} m^{-3} or high ion temperature higher than 4000 K is required. Therefore we assume that ions around the cusp region at an altitude of 630 km have been effectively heated/accelerated at energies above a few eV whereas the heating/acceleration has not been clearly shown in thermal energy ranges (at energies below a few eV).

[33] Let us now discuss what kind of mechanisms could heat ions only at energies above a few eV. In several

previous studies [*Norqvist et al.*, 1996; *André et al.*, 1998], wave-particle interaction has been a plausible candidate for the ion heating. There are no plasma wave data for our observations. As mentioned in the Introduction, Freja observations at altitudes of 1100–1600 km showed that ion energization perpendicular to the geomagnetic field dominates, and ions have mean energies of above 0.5 to a few eV in the cusp region [*Norqvist et al.*, 1998]. At the dayside including the cusp region, the perpendicular heating to a few eV can be frequently associated with weak broadband extremely low frequency (BBELF) wavefields [*Norqvist et al.*, 1996; *André et al.*, 1998]. These broadband waves cover frequencies from less than 1 Hz up to several times the oxygen gyrofrequency fo^+ at approximately 30 Hz. The resonant transfer of energy to O$^+$ ions from waves at frequencies in the order of fo^+ seems to be an important energization mechanism. The energization of the BBELF waves gives the highest average energies (up to hundreds of eV) and the largest upgoing number flux of ions [*André et al.*, 1998]. The SERSIO sounding rocket data also showed that 0–4 kHz BBELF wave activity was well correlated with the ion temperature enhancements up to 0.8 eV measured with the in situ measurement at the lower altitudes (520–780 km) [*Frederick-Frost et al.*, 2007].

[34] At an altitude of approximately 1600 km, the number of perpendicularly heated oxygen ions is very large compared with the number of detected protons, and the low-energy (less than 500 eV) downgoing electrons are correlated with the ion heating [*Norqvist et al.*, 1996]. These results also agree with ours at an altitude of approximately 630 km. Our observations indicate that the ions with a few eV energy move upward, anti-parallel to *B*, and that either the mirror force on perpendicular heated ions or a parallel electric field (or both) are acting below 630 km altitude accelerating ions upward. We do not know whether the ion distribution at energies around
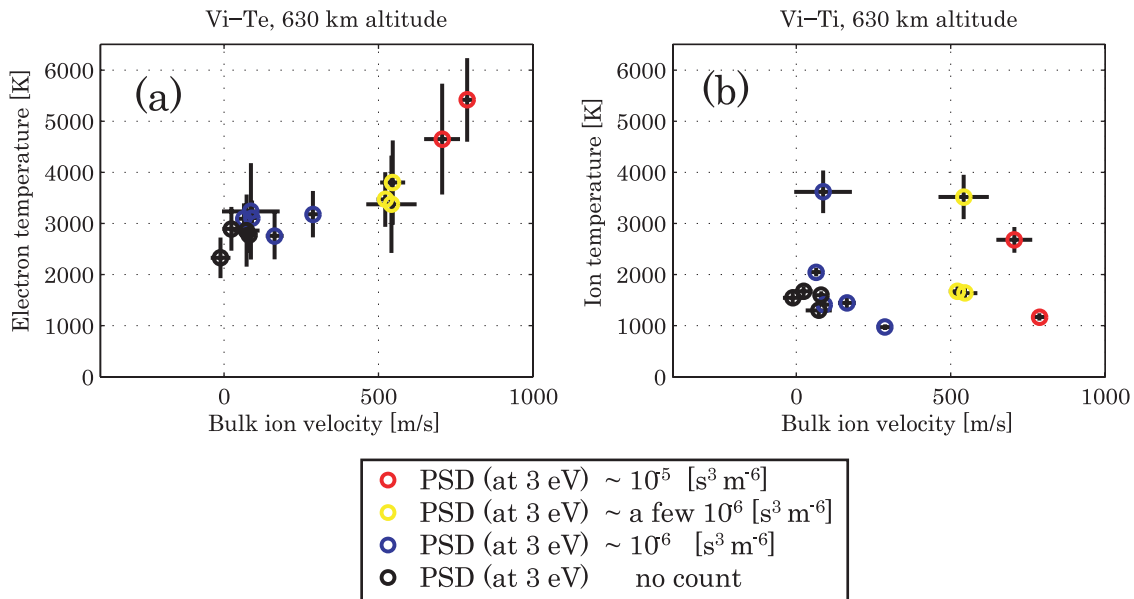

Figure 6. Relationship between the field-aligned (FA) bulk ion upflow and electron/ion temperature derived with the ESR 42m data. The 14 events are also binned into four groups (represented in the figure by overlays of red, yellow, blue, and black) according to the phase space density (PSD) of suprathermal ions in the direction perpendicular to the magnetic field, measured with Reimei.
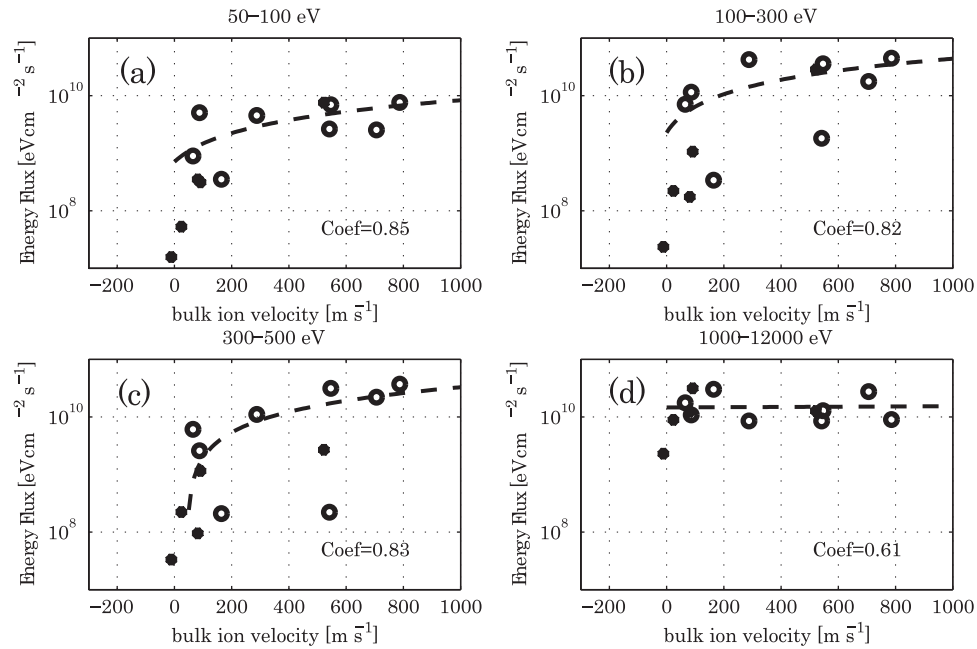
Figure 7. Energy fluxes of precipitating electrons (PA: 0−30 deg) as a function of the bulk ion velocity measured with the ESR. Corresponding energies of precipitating electrons are shown for (a) 50−100 eV, (b) 100−300 eV, (c) 300−500 eV, and (d) 1000−12,000 eV, respectively. Correlation coefficients are added in each plot. Open circles indicate samples obtained in November 2005, and black circles in August 2006.

a few eV is isotropic or anisotropic, because of limitations of Reimei ISA (see lack of the ISA data at energies below 10 eV along the field line in Figure 4b). This upflow of a few eV ions clearly corresponds to the bulk ion upflow and increase of the electron temperature due to soft electron precipitation. The results are consistent with those of the SIERRA rocket data analysis performed by *Lynch et al.* [2007]. *Lynch et al.* [2007] showed a clear relation between upflowing ions (<2 km/s) derived from 6 eV ions and soft electron precipitation (below 100 eV) and calculated using the TRANSCAR model that soft precipitation is more effective in initiating ion upflows than hard precipitation. On the basis of the results from the ESR and EISCAT Tromsø VHF data at an altitude of 665 km, *Ogawa et al.* [2000] also suggested that in addition to direct precipitation effects, namely enhanced ambipolar diffusion and heat flux, also wave-particle interaction, such as wave-induced transverse ion heating, which causes a hydrodynamic mirror force, may play a role in driving ion upflows.

[35] A case study, using data from 8 August 2006, shows the presence of naturally enhanced ion-acoustic lines (NEIALs). The NEIALs are a characteristic phenomenon of the cusp region [*Buchert et al.*, 1999; *Sedgemore-Schulthess et al.*, 1999; *Ogawa et al.*, 2006]. It is potentially important to understand the relation between BBELF waves (a few 10 Hz) and higher frequency turbulence, such as ion-acoustic turbulence (a few kHz), as well as Langmuir turbulence (a few MHz), and the contribution of higher frequency turbulence to energization of suprathermal ions with energy of a few eV. However, a detailed study of the waves lies outside the scope of this paper.

[36] In a collision-dominated region such as the *F* region ionosphere, Joule heating due to resonant charge exchange between O and O^+ is another heating process that produces an anisotropic ion velocity distribution. The Joule heating causes an increase of the FA ion temperature, as well as an increase of the ion temperature perpendicular to the magnetic field [e.g., *McCrea et al.*, 1993]. However, our results show that there was no correspondence between the FA ion temperature and the suprathermal ions, indicating that enhanced suprathermal ions in the cusp region were not associated with Joule heating.

[37] In addition to the suprathermal ions perpendicular or oblique to the magnetic field, those parallel to the magnetic field were also seen with energies of ∼10 eV (see Figure 4b). Such ions were not reported from satellite (such as the Freja satellite) observations at higher altitudes around 1000−2000 km, because the sunlight and very low-density plasma conditions cause heavily positive spacecraft potential (∼10 eV) and prevent observation of the low-energy ions. It is difficult to explain those suprathermal ions as a result of only wave-particle interaction, which causes heating perpendicular to the magnetic field. The suprathermal ions parallel to the magnetic field may be created by two different mechanisms, we propose. One is that the suprathermal ions perpendicular to the magnetic field become more isotropic at 630 km, via collisions between ions and neutrals, or coulomb collisions between ions and ions. The neutral density at 630 km altitude is more than a factor of 10 higher than that at 1600 km altitude, and therefore the collision frequency between ions and neutrals is also more than 10 times higher at 630 km. This might be a typical characteristic of suprathermal ion distributions at 630 km, where there is a transition from a collision-dominated region to a collisionless region. The other is that the satellite passed at the lower edge of an electric potential drop region, and

ions were accelerated upward up to 10 eV due to a parallel electric field [e.g., *Mozer*, 1980; *Boehm and Mozer*, 1981; *Min et al.*, 1993]. At the same time and location, precipitating electrons were accelerated by an upward parallel electric field up to around 200 eV along the magnetic field line.

5. Conclusions

[38] Coordinated Reimei satellite and EISCAT Svalbard radar (ESR) observations were conducted in November 2005 and August 2006, to investigate the relationship between thermal and suprathermal ion behavior in the dayside polar ionosphere. The results clarified the presence of suprathermal ions, with energies of a few eV, associated with the bulk ion upflows in the cusp region, even at an altitude of 630 km, which is close to the transition height from a collision-dominant region to a collisionless region. When we assume that velocity distributions of ions are Maxwellian or bi-Maxwellian, high temperatures (approximately 0.9 to 1.4 eV), derived from the suprathermal ions observed with the Reimei satellite, do not directly correspond to the ionospheric ion temperature (approximately 0.1 to 0.3 eV) observed with the ESR at the same time and altitude. This indicates that the ion velocity distributions have been heated at energies above a few eV in the cusp region.

[39] The increase of the phase space density (PSD) of low energy ions has a good correlation with the electron temperature increase caused by the soft electron precipitation, but not with the ion temperature (approximately 0.1–0.3 eV) at the same altitude derived using the ESR. As previous studies using the Freja satellite showed that ion cyclotron heating was caused by broadband extremely low frequency (BBELF) waves in the cusp region at approximately 1600 km altitude [e.g., *Norqvist et al.*, 1996], we suggest that the same ion cyclotron heating would occur at this lower altitude of 630 km in the cusp region, and therefore the heated ions would flow up to the magnetosphere. Our results also suggest that the ion temperature enhancements (up to 0.8 eV) measured with the SERSIO rocket and associated with the BBELF wave activity should be in the direction perpendicular or obliquely upward to the magnetic field.

[40] As mentioned in the Introduction, it is impossible to find the characteristics obtained in this study only from a single measurement. Our direct comparison of the IS radar and satellite data at the same time and altitude revealed the difference between the motions of thermal and suprathermal ions. Further simultaneous observations will be focused on thermal ion energization and related plasma fluctuation/turbulence. The current probes (CRM) data on the Reimei has the potential to proceed to the next investigation. The payload disturbances on the low energy ion data will be carefully investigated with the CRM data.

References

André, M. (1997), Waves and wave-particle interactions in the auroral region, *J. Atmos. Terr. Phys.*, 59, 1687–1712.

André, M., P. Norqvist, L. Andersson, L. Eliasson, A. I. Eriksson, L. Blomberg, R. E. Erlandson, and J. Waldemark (1998), Ion energization mechanisms at 1700 km in the auroral region, *J. Geophys. Res.*, 103(A3), 4199–4222.

Asamura, K., D. Tsujita, H. Tanaka, Y. Saito, T. Mukai, and M. Hirahara (2003), Auroral particle instrument onboard the INDEX satellite, *Adv. Space Res.*, 32, 375–378.

Boehm, M. H., and F. S. Mozer (1981), An S3-3 search for confined regions of large parallel electric fields, *Geophys. Res. Lett.*, 8(6), 607–610.

Buchert, S. C., A. P. van Eyken, T. Ogawa, and S. Watanabe (1999), Naturally enhanced ion-acoustic lines seen with the EISCAT Svalbard Radar, *Adv. Space Res.*, 23, 1699–1704.

Endo, M., R. Fujii, Y. Ogawa, S. C. Buchert, S. Nozawa, S. Watanabe, and N. Yoshida (2000), Ion upflow and downflow at the topside ionosphere observed by the EISCAT VHF radar, *Ann. Geophys.*, 18, 170–181.

Foster, C., M. Lester, and J. A. Davies (1998), A statistical study of diurnal, seasonal and solar cycle variations of F-region and topside auroral upflows observed by EISCAT between 1984 and 1996, *Ann. Geophys.*, 16, 1144–1158.

Frederick-Frost, K. M., K. A. Lynch, P. M. Kintner, E. Klatt, D. Lorentzen, J. Moen, Y. Ogawa, and M. Widholm (2007), SERSIO: Svalbard EISCAT rocket study of ion outflows, *J. Geophys. Res.*, 112, A08307, doi:10.1029/2006JA011942.

Hultqvist, B. (1996), On the acceleration of positive ions by high-latitude, large-amplitude electric field fluctuations, *J. Geophys. Res.*, 101(A12), 27,111–27,121.

Keating, J. G., F. J. Mulligan, D. B. Doyle, K. J. Winser, and M. Lockwood (1990), A statistical study of large field-aligned flows of thermal ions at high-latitudes, *Planet. Space Sci.*, 38, 1187–1201.

Kintner, P. M., J. Bonnell, R. Arnoldy, K. Lynch, C. Pollock, and T. Moore (1996), SCIFER-Transverse ion acceleration and plasma waves, *Geophys. Res. Lett.*, 23(14), 1873–1876.

Lundin, R., and B. Hultqvist (1989), Ionospheric plasma escape by high-altitude electric fields — Magnetic moment "pumping", *J. Geophys. Res.*, 94(A6), 6665–6680.

Lynch, K. A., R. L. Arnoldy, P. M. Kintner, and J. Bonnell (1996), The AMICIST auroral sounding rocket: A comparison of transverse ion acceleration mechanisms, *Geophys. Res. Lett.*, 23(23), 3293–3296.

Lynch, K. A., J. L. Semeter, M. Zettergren, P. Kintner, R. Arnoldy, E. Klatt, J. LaBelle, R. G. Michell, E. A. MacDonald, and M. Samara (2007), Auroral ion outflow: Low altitude energization, *Ann. Geophys.*, 25, 1967–1977.

Maynard, N. C., E. J. Weber, D. R. Weimer, J. Moen, T. Onsager, R. A. Heelis, and A. Egeland (1997), How wide in magnetic local time is the cusp? An event study, *J. Geophys. Res.*, 102(A3), 4765–4776.

McCrea, I. W., M. Lester, T. R. Robinson, J.-P. St.-Maurice, N. M. Wade, and T. B. Jones (1993), Derivation of the ion temperature partition coefficient beta-parallel from the study of ion frictional heating events, *J. Geophys. Res.*, 98(A9), 15,701–15,715.

Min, Q.-L., D. Lummerzheim, M. H. Rees, and K. Stamnes (1993), Effects of a parallel electric field and the geomagnetic field in the topside ionosphere on auroral and photoelectron energy distributions, *J. Geophys. Res.*, 98(A11), 19,223–19,234.

Moore, T. E., C. J. Pollock, M. L. Adrian, P. M. Kintner, R. L. Arnoldy, K. A. Lynch, and J. A. Holtet (1996), The cleft ion plasma environment at low solar activity, *Geophys. Res. Lett.*, 23(14), 1877–1880.

Mozer, F. S. (1980), On the lowest altitude S3-3 observations of electrostatic shocks and parallel electric fields, *Geophys. Res. Lett.*, 7(12), 1097–1100.

Newell, P. T., and C.-I. Meng (1992), Mapping the dayside ionosphere to the magnetosphere according to particle precipitation characteristics, *Geophys. Res. Lett.*, 19(6), 609–612.

Norqvist, P., M. André, L. Eliasson, A. I. Eriksson, L. Blomberg, H. Lühr, and J. H. Clemmons (1996), Ion cyclotron heating in the dayside magnetosphere, *J. Geophys. Res.*, 101, 13,179–13,194.

Norqvist, P., T. Oscarsson, M. André, and L. Blomberg (1998), Isotropic and perpendicular energization of oxygen ions at energies below 1 eV, *J. Geophys. Res.*, 103(A3), 4223–4239.

Ogawa, Y., R. Fujii, S. C. Buchert, S. Nozawa, S. Watanabe, and A. P. van Eyken (2000), Simultaneous EISCAT Svalbard and VHF radar

observations of ion upflows at different aspect angles, *Geophys. Res. Lett.*, *27*(1), 81–84.

Ogawa, Y., R. Fujii, S. C. Buchert, S. Nozawa, and S. Ohtani (2003), Simultaneous EISCAT Svalbard radar and DMSP observations of ion upflow in the dayside ionosphere, *J. Geophys. Res.*, *108*(A3), 1101, doi:10.1029/2002JA009590.

Ogawa, Y., S. C. Buchert, R. Fujii, S. Nozawa, and F. Forme (2006), Naturally enhanced ion-acoustic lines at high altitudes, *Ann. Geophys.*, *24*, 3351–3364.

Saito, H., et al. (2005), An-overview and initital in-orbit status of "INDEX" satellite, *56th International Astronautical Confernce*, IAC-05-B5.6.B.05.

Sakanoi, T., S. Okano, Y. Obuchi, T. Kobayashi, M. Ejiri, K. Asamura, and M. Hirahara (2003), Development of the multi-spectral auroral camera onboard the INDEX satellite, *Adv. Space Res.*, *32*, 379–384.

Sedgemore-Schulthess, K. J. F., M. Lockwood, T. S. Trondsen, B. S. Lanchester, M. H. Rees, D. A. Lorentzen, and J. Moen (1999), Coherent EISCAT Svalbard Radar spectra from the dayside cusp/cleft and their implications for transient field-aligned currents, *J. Geophys. Res.*, *104*(A11), 24,613–24,624.

Wahlund, J.-E., H. J. Opgenoorth, I. Häggström, K. J. Winser, and G. O. L. Jones (1992), EISCAT observations of topside ionospheric ion outflows during auroral activity: Revisited, *J. Geophys. Res.*, *97*(A3), 3019–3037.

————————————

K. Asamura and A. Yamazaki, Institute of Space and Astronautical Science, Japan Aerospace Exploration Agency, 3-1-1 Yoshinodai, Sagamihara, Kanagawa, 229-8510 Japan.

S. C. Buchert, Swedish Institute of Space Physics, Box 537, SE-75121 Uppsala, Sweden.

Y. Ebihara, Institute for Advanced Research, Nagoya University, Chikusa-ku, Foro-cho, Nagoya, 464-8601 Japan.

R. Fujii, S. Nozawa, and K. Seki, Solar-Terrestrial Environment Laboratory, Nagoya University, Foro-cho, Chikusa-ku, Nagoya, 464-8601 Japan.

M. Hirahara, Department of Physics, College of Science, Rikkyo University, 3-34-1 Nishiikebukuro, Toyoshima-ku, Tokyo, 171-8501 Japan.

Y. Obuchi and T. Sakanoi, Planetary Plasma and Atmospheric Research Center, Graduate School of Science, Tohoku University, 28 Kawauchi, Aoba-ku, Sendai, 980-8576 Japan.

Y. Ogawa, National Institute of Polar Research, 1-9-10 Kaga, Itabashi-ku, Tokyo, 173-8515 Japan. (yogawa@nipr.ac.jp)

I. Sandahl, Swedish Institute of Space Physics, Box 812, SE-98128 Kiruna, Sweden.